Supernova Explosions and the Birth of Neutron Stars

H.-Thomas Janka, Andreas Marek, Bernhard Müller and Leonhard Scheck

Max Planck Institute for Astrophysics, Karl-Schwarzschild-Str. 1, D-85741 Garching, Germany

Abstract. We report here on recent progress in understanding the birth conditions of neutron stars and the way how supernovae explode. More sophisticated numerical models have led to the discovery of new phenomena in the supernova core, for example a generic hydrodynamic instability of the stagnant supernova shock against low-mode nonradial deformation and the excitation of gravity-wave activity in the surface and core of the nascent neutron star. Both can have supportive or decisive influence on the inauguration of the explosion, the former by improving the conditions for energy deposition by neutrino heating in the postshock gas, the latter by supplying the developing blast with a flux of acoustic power that adds to the energy transfer by neutrinos. While recent two-dimensional models suggest that the neutrino-driven mechanism may be viable for stars from $\sim 8\,M_\odot$ to at least $15\,M_\odot$, acoustic energy input has been advocated as an alternative if neutrino heating fails. Magnetohydrodynamic effects constitute another way to trigger explosions in connection with the collapse of sufficiently rapidly rotating stellar cores, perhaps linked to the birth of magnetars. The global explosion asymmetries seen in the recent simulations offer an explanation of even the highest measured kick velocities of young neutron stars.

Keywords: supernovae, explosion mechanisms, pulsar kicks
PACS: 97.60.Bw, 97.60.Jd

INTRODUCTION

Improved numerical tools and the increasing power of modern supercomputers have brought considerable progress in modeling stellar core collapse in the past years. It is possible now to simulate the complex physical processes in the deep interior of supernovae with unprecedented sophistication and detailedness.

It has become clear meanwhile that the explosions of massive stars are a generically multi-dimensional phenomenon. This insight was fostered by the fact that spherically symmetric (1D) simulations, which became available with a fully energy dependent solution of the Boltzmann transport problem for the neutrinos only recently (see [1] for an overview and comparison of different numerical approaches) confirmed and solidified older 1D results of the 1980's and 1990's, namely that explosions in the 1D models could not be obtained, neither by the prompt bounce-shock nor by the delayed neutrino-heating mechanism, at least not for progenitor stars of more than $10\,M_\odot$ and on a timescale of roughly one second after core bounce [2, 3, 4, 5]. Moreover, the latest generation of multi-dimensional simulations has provided evidence for a variety of routes that can lead to explosions when nonradial phenomena are accounted for. These routes seem to depend on the properties and conditions in the progenitor stars like their mass and structure and the amount of angular momentum in their core.

In the following we will briefly review these recent developments in the multi-dimensional modeling of stellar core collapse and explosion, and we will critically discuss the status of the present simulations.

A better understanding of the explosion mechanism of core-collapse supernovae is not only important for interpreting the observable properties of the blast, for predicting gravitational-wave and neutrino signals, and for determining the conditions of nucleosynthesis processes that occur during the explosion. It is also and in particular essential for establishing the link between the progenitor stars and their compact remnants, thus answering questions like that of the mass distribution of neutron stars and of the stellar mass limit for black hole formation, which may happen either directly during the core collapse or by later massive fallback when the disrupted star does not become completely unbound during the explosion. So far, estimates for such scenarios have been made only on the basis of still rather crude self-consistent explosion simulations [6] or by invoking assumptions about the mass cut and energy in models with piston-driven artificial explosions (e.g., [7]).

BRIEF HISTORICAL EXCURSION

Due to the huge gravitational binding energy liberated in neutrinos, which carry away hundred times more energy than needed for the explosion, these particles have long been speculated to be the driving agent of the stellar explosion. Colgate and White [8] in a seminal paper in 1966 not only proposed gravitational binding energy to be the primary energy source of core-collapse supernovae, but also that the intense flux of escaping neutrinos transfers the energy from the imploding core to the ejected stellar mantle. Nearly twenty years later, Bethe

and Wilson [9] were the first who described in detail the way how this might happen, interpeting thereby the physics that played a role in hydrodynamic simulations performed by Wilson. They concluded that electron neutrino and antineutrino absorptions on the free neutrons and protons that are abundantly present in the shock-dissociated matter behind the stalled accretion shock in the supernova core, are the primary agents of the energy transfer.

These pioneering computer simulations of the so-called delayed neutrino-driven explosion mechanism were still conducted in spherical symmetry. The mechanism turned out to be successful only when the neutron star was assumed to become a more luminous neutrino source by mixing instabilities accelerating the energy transport out of its dense interior. The thus enhanced neutrino emission led to stronger neutrino heating in the overlying layers of the exploding star. Theoretical studies and multi-dimensional computer models, however, suggest that convection and mixing instabilities inside the neutron star do not have the necessary big effect (see, e.g. [10, 3, 11, 12]). Instead, the first multi-dimensional simulations, which became available only in the mid 1990's, demonstrated that the neutrino-heated layer around the forming neutron star is unstable to vigorous convective overturn [13, 14, 15, 6, 16, 17]. This can raise the efficiency of the neutrino energy deposition and thus can have a supportive effect on the supernova explosion. The first such two-dimensional (i.e. axisymmetric) and three-dimensional simulations, however, suffered from a severe drawback: the physics of the neutrino transport and of neutrino-matter interactions, which is essential for discussing the power input to the explosion, is so complex that it could be treated only in a grossly simplified way. In the best models at that time this was done by the so-called "grey diffusion approximation". This means that the energy-dependence of the neutrino interactions (the cross sections of the most important neutrino processes typically scale with the squared neutrino energy) was ignored and replaced by a "grey" (spectrally averaged) description. Moreover, the spatial propagation was approximated by assuming that neutrinos diffuse through the dense neutron star medium until they decouple and stream away from a chosen position, usually from a layer somewhat outside of the "neutrinosphere", close to the surface of the compact remnant. The historical development of these theoretical studies of the supernova explosion mechanism is resumed in a recent review [18].

RECENT RESULTS

Only in the past years the neutrino treatment in multi-dimensional hydrodynamic and magnetohydrodynamic (MHD) models of supernovae has seen significant improvements. However, a rigorous solution of the Boltzmann transport equation is still much too time consuming to be applied in full-scale simulations. Even in axially symmetric (2D) models the transport poses a five-dimensional problem (see, e.g., [20]), in three dimensional hydrodynamic simulations it would constitute a time-dependent six-dimensional problem.

All active groups therefore still have to accept some simplifications and nevertheless the neutrino transport module dominates the computing time for supernova simulations by far. The approximations taken by different groups differ significantly. While the Tucson-Jerusalem collaboration employs a 2D flux-limited diffusion scheme and treats the neutrino energy groups uncoupled (an approach that is known from 1D simulations to be unable to capture important physics), thus gaining a modest amount of straightforward parallelism for their computations (e.g., [21, 22, 23], the transport treatment of the Garching group accounts for the full energy dependence of the problem and solves on each angular (lateral) bin of the 2D grid a full one-dimensional transport problem by iterating the moment equations of neutrino number, energy, and momentum with a variable Eddington factor for the closure that is obtained from the solution of a model Boltzmann equation. Moreover, neutrino pressure gradients and advection in the lateral direction are included in this so-called "ray-by-ray plus" approximation [24, 25]. While this approach assumes that the neutrino flux components in lateral direction are zero (i.e., the neutrino intensity is taken to be symmetric around the radial direction), it allows one to properly treat the gradual transition of neutrinos from diffusion at the high densities in the neutron star interior to free streaming in the much more dilute stellar layers far outside of the neutron star. This approach has also the big advantage of being a direct generalization of the 1D case and therefore it enables a detailed, well constrained comparison of 1D and 2D simulations.

In the following we will summarize the essentials of recent two-dimensional studies that have made use of the mentioned improvements in the neutrino transport, and which have thus contributed to a better understanding of the question how the collapse of stellar cores could be reversed to an explosion. The basic requirement for this to happen is that some energy reservoir that takes up gravitational binding energy released during stellar core collapse can be effectively tapped and transferred to matter that can get expelled in the explosion. This can happen by neutrinos in the context of the neutrino-heating mechanism, but it can also be achieved by magnetic fields in magnetohydrodynamic (MHD) explosions. Or it may occur, as recently proposed [21, 22], through sound waves created by violently turbulent gas motions around the impact sites of accretion downflows on the neutron star surface, or even by large-amplitude g-mode pulsations of

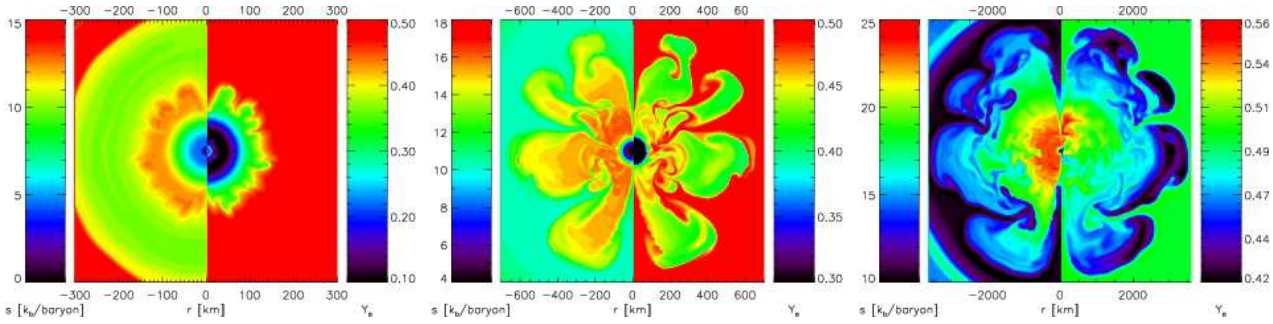

FIGURE 1. Snaphots showing the gas entropy (left half of panels) and the electron-to-nucleon ratio (right half of panels) for the explosion of an $\sim 9\,M_\odot$ star with an O-Ne-Mg core. The plots correspond (from top left to bottom right) to times of 0.097, 0.144, and 0.262 seconds after the launch of the supernova shock front and the onset of neutron star formation at the moment of core bounce. Note the different radial and color scales of the four panels. Due to the rapid expansion of the shock and of the shock-accelerated ejecta into the extremely dilute layers surrounding the O-Ne-Mg core, the convective pattern freezes out quickly and begins a nearly self-similar expansion. The characteristic wavelength of convective structures is roughly 30–45 degrees (corresponding to dominant spherical harmonics modes of $l = 4, 5$) and there is no strong contribution of dipolar and quadrupolar asymmetries.

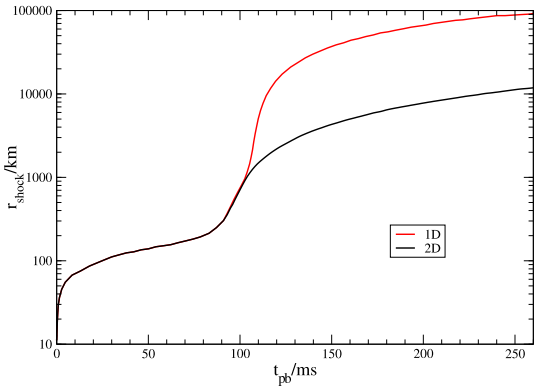

FIGURE 2. Radii of the supernova shock as functions of time for one- and two-dimensional simulations (red and black lines, respectively) of the explosion of a star with O-Ne-Mg core. Note that the progenitor used in the 2D simulation was an $8.8\,M_\odot$ model with an artificially constructed low-density He-shell at $\rho < 10^3\,\mathrm{g\,cm^{-3}}$ [19], while the 1D simulation was performed with a recently updated progenitor structure in which a H-envelope with a much lower density and steeper density decline was added around the O-Ne-Mg core (K. Nomoto, private communication). This explains the stronger acceleration of the shock in the region outside of about 1100 km.

the neutron star core, leading to acoustically powered explosions.

Neutrino-driven explosions

Neutrinos extract energy from the huge reservoir of degeneracy and thermal energy that is built up inside of the nascent neutron star during stellar core collapse. These neutrinos diffuse out of the dense interior and before streaming off to low-density regions, mostly neutrinos of the electron flavor deposit roughly 10% of their energy in the so-called gain layer between the gain radius and the stalled supernova shock. Detailed and accurate numerical models are indispensable to determine the exact efficiency of this energy transfer.

Results obtained by the Garching group for progenitor stars between 9 and 15 solar masses confirm the viability of the neutrino-heating mechanism for triggering supernova explosions. However, the inauguration of the explosion happens in a different way than expected from previous models and the blast properties turn out to differ significantly from older calculations with more simplified neutrino physics.

Supernova progenitors with less than about $10\,M_\odot$ clearly vary in their structure and explosion behavior from more massive stars. The former class of stars develops a core composed of oxygen, neon, and magnesium, not of iron, with an extremely steep density gradient at its surface. This allows the supernova shock front, which is launched at the moment when the neutron star begins to form at the center of the collapsing stellar core, to expand continuously as it propagates into rapidly diluting infalling material. Behind the shock the velocities are initially negative, so that no prompt explosion occurs. But then neutrino heating deposits the energy that powers the ensuing blast. Convective overturn develops in the neutrino-heated layer behind the outgoing shock and imprints inhomogeneities on the ejecta, in entropy as well as composition (Fig. 1). But because of the rapid acceleration of the supernova shock and of the postshock layer (Fig. 2), the pattern of Rayleigh-Taylor structures freezes out quickly (when the expansion timescale becomes shorter than the overturn timescale) and the inhomogeneous shell behind the shock begins an essentially self-similar expansion. The short convective phase leads to large-scale explosion asymmetries, however, without

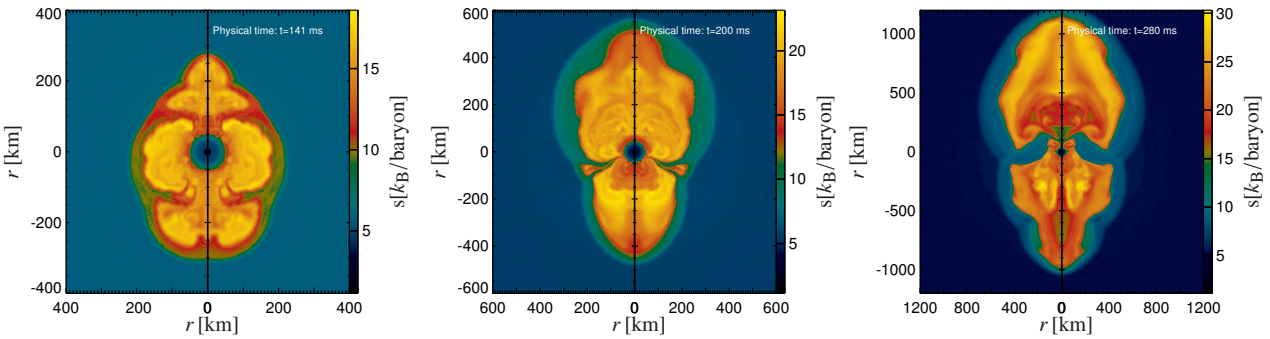

FIGURE 3. Snapshots of the gas entropy for the explosion of a star with $11.2\,M_\odot$ at times 0.14, 0.20, and 0.28 seconds after the launch of the supernova shock at core bounce (top left to bottom right). The explosion develops a large bipolar asymmetry although the star is not rotating. Note the different radial and entropy scales of the four panels. The first two plots show results from Ref. [3], the last one is from a recent continuation of the same simulation to later times.

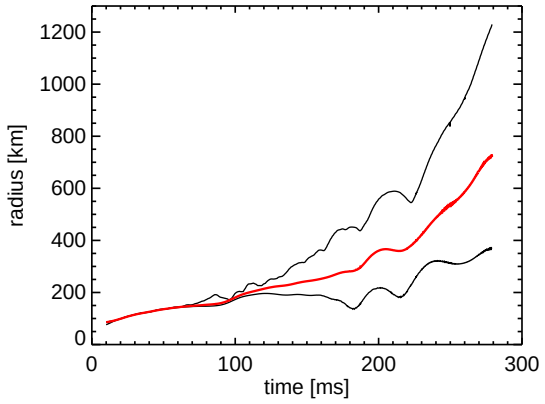

FIGURE 4. Maximum, average, and minimum radial position of the supernova shock front as functions of time for the explosion of the $11.2\,M_\odot$ model displayed in Fig. 3. Note the clear signature of several large-amplitude bipolar shock oscillations due to the standing accretion shock instability (SASI) before the blast takes off with an extreme 3:1 deformation.

global dipolar or quadrupolar deformation (Fig. 1).

Evolved stars above roughly $10\,M_\odot$ produce iron cores with a much more shallow density decline outside. Running into this denser material damps the initial expansion of the shock. Moreover, severe energy losses and the high mass infall rates cause the shock to even stall at a relatively small radius of only about 100 km. Because of the small shock stagnation radius, the infall velocities of the collapsing stellar core ahead and behind the shock are very large. Different from previous calculations with simple grey neutrino diffusion, our more sophisticated models show that convection is strongly suppressed in the rapidly infalling matter behind the shock. Neutrino heating is not powerful enough to allow high-entropy matter to become buoyant against the accretion flow (see [26, 27]). Convective overturn behind the shock therefore cannot become sufficiently strong to help pushing the stagnant shock farther out and thus to establish more favorable conditions for neutrino heating.

Instead, another kind of nonradial hydrodynamic instability, the so-called standing accretion shock instability ("SASI"; [28]), which can grow efficiently even when convection stays weak [29, 30, 27], obtains decisive influence on the shock evolution. With highest growth rates of the dipole and quadrupole modes [31], it leads to violent bipolar sloshing motions of the shock. This drives the shock front to larger radii and thus reduces the accretion velocities in the postshock layer. The obliqueness of the shock surface relative to the infalling stellar core material deflects the accretion flow and stretches its path through the layer of neutrino heating. Moreover, the SASI also causes secondary convection due to steep entropy gradients produced in the postshock layer by the quasi-periodic expansion and contraction phases of the shock. The influence of the SASI thus improves the conditions for efficient energy deposition by neutrinos, because the gas accreted through the stalled shock can stay longer in the heating layer and is therefore able to absorb more energy from the intense neutrino flux radiated by the nascent neutron star [27].

The presence of strong SASI oscillations is visible in simulations for an $11.2\,M_\odot$ star (for details, see [3]) and for a $15\,M_\odot$ star (details in Ref. [32]). The SASI turns out to be crucial for the explosion in both cases (Figs. 3–5). Different from the $\sim 9\,M_\odot$ star, where convection imposes a high-mode asymmetry pattern on the ejecta (see Fig. 1), the preferred growth of the dipole and quadrupole ($l = 1, 2$; $m = 0$ in terms of an expansion of the characteristic flow properties in spherical harmonics) modes of the SASI leads to a large global anisotropy of the beginning supernova blast in the more massive progenitors.

Our simulations have thus demonstrated the decisive role of the standing accretion shock instability in combination with neutrino heating for initiating neutrino-powered supernovae. The explosion may set in with a

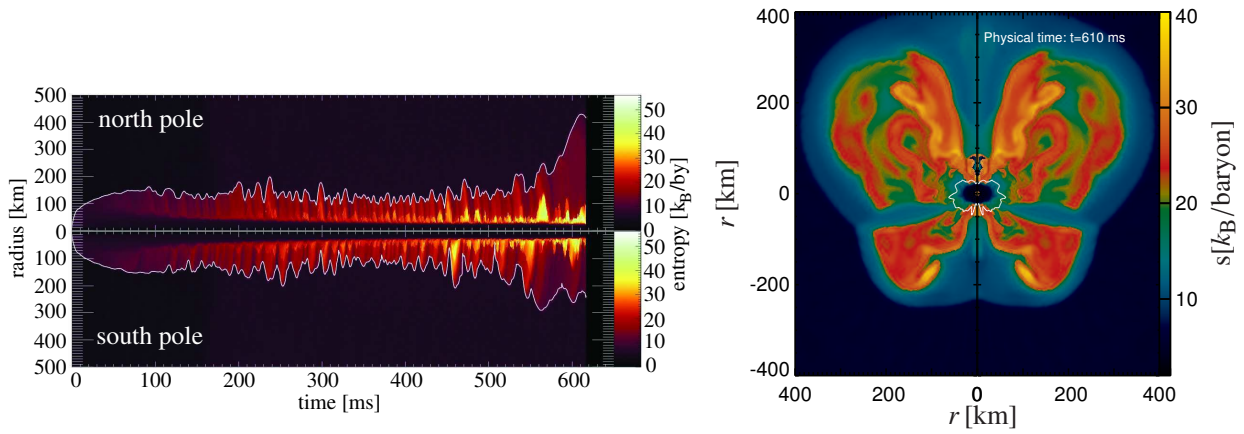

FIGURE 5. *Left:* Shock positions near the north pole and near the south pole as functions of time for a $15\,M_\odot$ star that evolves towards the onset of an explosion at >600 ms after core bounce. The gas entropy is color coded. The plot shows many cycles of quasi-periodic bipolar shock oscillations due to the standing accretion shock instability (SASI). *Right:* Gas entropy distribution for the $15\,M_\odot$ star at the onset of the explosion at a time of 0.61 s after bounce. A large north-south asymmetry signals a strong contribution from the dipole mode. The white line marks the gain radius as lower boundary of the neutrino-heating region (both plots are from [32]).

TABLE 1. Estimated explosion properties for different progenitor stars with ZAMS mass $M_{\rm prog}$

$M_{\rm prog}$ $[M_\odot]$	$t_{\rm expl}$ * [ms]	$M_{\rm acc}$ † $[M_\odot]$	$E_{\rm expl}$ ** [B]	$M_{\rm ns,b}$ ‡ $[M_\odot]$
$\sim$9	120	0.01–0.02	0.2–0.3	1.36
11.2	220	0.02–0.04	0.3–0.6	1.30
15	620	0.05–0.06	$\sim$1.0	1.55

* Time of onset of explosion, determined as the moment when the total energy in the gain layer, integrated over the mass elements with positive specific total energy, exceeds 10^{49} erg

† Mass of accreted, neutrino-heated, and then ejected matter accounting for the explosion energy estimate of Eq. (1)

** Explosion energy estimated according to Eq. (1) in $1\,{\rm B} = 1\,{\rm bethe} = 10^{51}$ erg

‡ Baryonic mass of the neutron star at the onset of the explosion

significant delay after the neutron star begins to form (similar results, however with Newtonian gravity instead of a relativistic gravitational potential were recently reported in Ref. [33]). For the most massive of the three investigated stars this happens about 0.6 seconds later. This is not only much later than expected from previous simulations, but also constitutes a major computational challenge for our 2D modeling with sophisticated multi-energy-group neutrino transport, for which reason our set of computed cases is still constrained to only three progenitors.

Table 1 summarizes the prediced explosion and remnant properties for these three progenitors. Only in the case of the rapidly developing blast of the $\sim 9\,M_\odot$ star could the 1D and 2D calculations be carried on for a sufficiently long time to see the explosion energy asymptote. For the other two models the explosion energy is built up during a possibly long-lasting phase of anisotropic accretion and simultaneous expansion of neutrino-heated matter, which is a manifestation of the multi-dimensional nature of the explosion [34, 22, 23, 12]. The explosion energy can then be roughly estimated from (for details, see [32])

$$E_{\rm exp} \sim \dot{E}_\nu\,\tau_{\rm acc} \sim M_{\rm acc}\,e_\nu\,, \qquad (1)$$

where $\dot{E}_\nu$ is the net (i.e., heating minus cooling) neutrino energy transfer rate to accreted and ejected gas,

$$\dot{E}_\nu \sim \zeta \dot{M}_{\rm acc}\,e_\nu \sim 2\times 10^{51}\,\frac{\rm erg}{\rm s}\,, \qquad (2)$$

when $\dot{M}_{\rm acc} \sim 0.2\,M_\odot/{\rm s}$ is the mass accretion rate through the shock when the explosion begins in the 11.2 and $15\,M_\odot$ models, $\zeta \sim 0.5$ is the fraction of the accreted gas that gets ejected again after being heated by neutrinos, $e_\nu \sim 10\,{\rm MeV/nucleon} \sim 10^{19}\,{\rm erg/g}$ is the average specific energy deposited by neutrinos in the gas, and $M_{\rm acc} = \zeta \dot{M}_{\rm acc}\,\tau_{\rm acc}$ is the accreted and subsequently expelled gas mass. Accretion can continue until the post-shock matter is accelerated to escape velocity by the outgoing shock, which leads to an estimate of the accretion time as $\tau_{\rm acc} \sim 0.5\,{\rm s}\,M_{\rm ns,1.5}\,v_{\rm sh,9}^{-3}$, when $M_{\rm ns,1.5}$ is the neutron star mass normalized to $1.5\,M_\odot$ and $v_{\rm sh,9}$ is the shock velocity in units of 10^9 cm/s (see [32]).

The non-monotonic behavior of the initial neutron star (baryonic) mass is linked to the core size of the progenitors and the surrounding density structure, because the latter determines the delay of the explosion and the duration of the accretion phase after bounce.

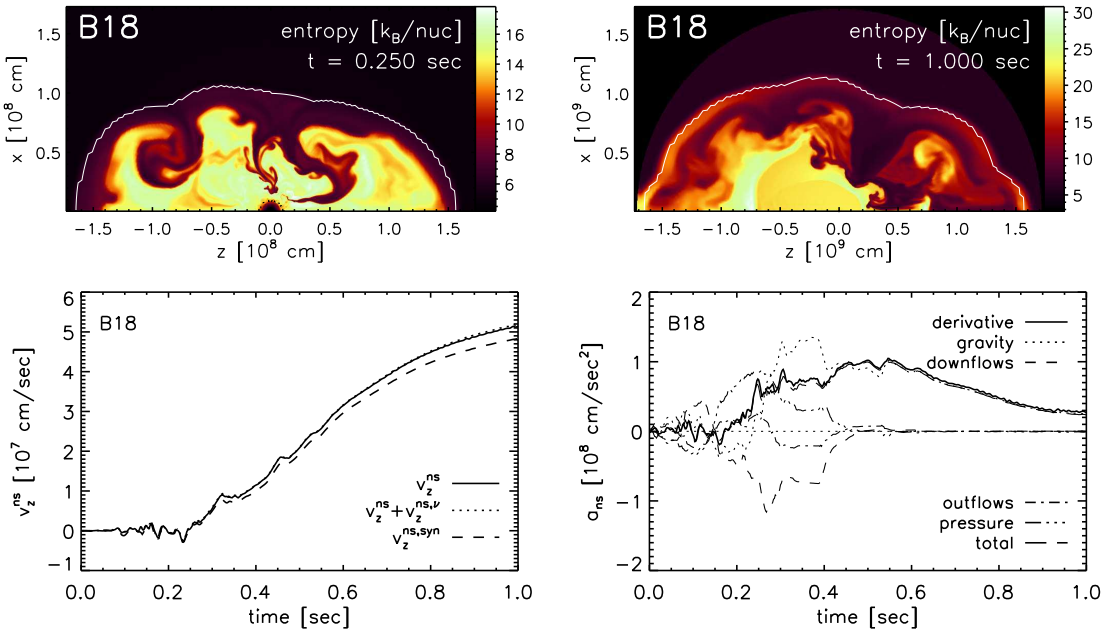

FIGURE 6. *Upper panels:* Two snapshots of the entropy distribution at 0.25 s and 1.0 s after bounce for one of the simulations in Ref. [34]. The anisotropic ejecta distribution leads to a neutron star kick as explained in the text. *Lower panels:* Neutron star recoil velocity (left) and acceleration (right) as functions of time after bounce for the simulation shown in the upper two panels. The solid curves are the result deduced directly from the hydrodynamic simulation, the dashed curve in the left plot and the long-dashed curve in the right plot are from an independent post-processing analysis of all accelerating effects on the neutron star. It turns out that the gravitational pull of the anisotropic ejecta is the main mediator of the neutron star acceleration at $t > 0.5$ s (dotted curve in the right panel) and dominates anisotropic accretion and outflows and pressure forces (short-dashed, dash-dotted, and dashed-triple dotted, respectively, in the right panel) by far. Anisotropic neutrino emission has usually a small influence (difference between solid and dotted lines in the left panel).

Explosion asymmetries and pulsar kicks

One of the consequences of this SASI-supported neutrino-driven mechanism is a global asymmetry of the accelerating shock front and of the ejected gas even in the absence of rotation (or with only very little rotation) in the stellar core. When the dipole and quadrupole modes are very strong, the onset of the explosion can resemble even a bipolar jet-like blast with a sizable pole-to-equator deformation (see Figs. 3 and 4).

A strongly deformed shock wave triggers mixing instabilities (Rayleigh-Taylor as well as Richtmyer-Meshkov) at the interfaces of the different composition shells of the exploding star after the passage of the outgoing shock wave. This was shown to lead to large-scale mixing of the chemical elements between the deep interior and the outer stellar layers during the explosion, explaining self-consistently a variety of properties observed in well-monitored supernovae like the famous Supernova 1987A, for example the high nickel velocities, the inhomogeneous and clumpy distribution of the metals, and the spreading of hydrogen over a wide range of velocities that had to be invoked for explaining the smoothness and broadness of the lightcurve peak [35]. Big explosion asymmetries can therefore not be interpreted as a signature of MHD-driven ("jet-driven") explosions.

Scheck et al. [34], performing a large set of 2D simulations for neutrino-driven explosions with an approximative description of the neutrino transport and using the neutrino luminosities from the contracting and cooling neutron star as a parametric boundary condition, showed that such large explosion asymmetries can leave the compact remnant with recoil velocities sufficiently large to explain the measured eigenvelocities of young pulsars. In cases where a dipolar asymmetry became dominant and the explosion developed more strength in one hemisphere than in the other, typical kick velocities around 500 km/s were found, with peak values even above 1000 km/s, whereas in cases where the higher modes were stronger than the $l = 1$ asymmetry, the velocities stayed fairly modest, usually below about 200 km/s (see Fig. 20 in [34]).

The pulsar recoil is caused by the asymmetry which the SASI distorted explosion develops on the long run, i.e. over a timescale of many seconds. During the on-

set of the explosion, even until the shock reaches a radius of some 1000 km, the pulsar kick usually does not grow to large values, which indicates that the ejecta have not obtained a high momentum asymmetry until then. In Fig. 6, which displays one of the cases computed in Ref. [34], the left panels show that the neutron star is essentially not accelerated until 250 ms after bounce when the maximum shock radius in this simulation is beyond 1500 km, and even at 400 ms post bounce the neutron star has attained a velocity of less than 100 km/s. Only later the acceleration grows and leads to a recoil velocity that asymptotes much after one second post bounce. The reason for such a long-lasting neutron star propulsion can neither be anisotropic accretion nor anisotropic mass ejection in the neutrino-driven wind. The former ceases at about 0.5 s p.b., while the neutrino wind is essentially spherically symmetric, corresponding to a neutrino emission that is nearly isotropic and thus also produces only a very small effect on the neutron star kick velocity (see left lower panel of Fig. 6).

A careful analysis of all effects that can transfer momentum between the surrounding gas and the compact remnant, i.e., gas outflow and accetion, anisotropic pressure, neutrino emission, and gravitational forces, shows that mostly the last mediate the speed-up of the neutron star at $t > 0.4$ s, whereas before that time all individual forces are large but nearly balanced (see lower right panel of Fig. 6 and for details, Ref. [34]). The explosion asymmetries, which are the cause of the gravitational momentum transfer to the neutron star, develop only gradually when the outward moving shock encompasses more and more matter from the progenitor star. Since the shock was launched highly aspherically as a result of the SASI motions, the gas swept up by the shock may not experience the same acceleration everywhere. If the shock is weaker in a certain direction or is oblique to the radius vector, the swept up gas is less strongly accelerated. This slower gas begins to lag behind the ejecta expanding in other directions. It is funneled into dense, downward-reaching, low-entropy filaments with the typical mushroom-like Rayleigh-Taylor caps (these are visible in the right upper panel of Fig. 6). The gravitational attraction of such massive gas pockets, which are closer to the neutron star than the ejecta in other directions, excerts an anisotropic pull on the compact remnant. Reversely, this pull decelerates the still expanding gas, thus transferring some of the ejecta momentum to the neutron star. In the extreme case, the gas may be gravitationally captured and may fall back to be accreted by the neutron star. The acceleration ceases and the neutron star speed asymptotes, when the inhomogeneous ejecta reach larger and larger radii and the anisotropic gravitational forces diminish. As a consequence of this acceleration, the neutron star motion is predicted to be opposite to the main momentum of the matter ejected in the supernova blast.

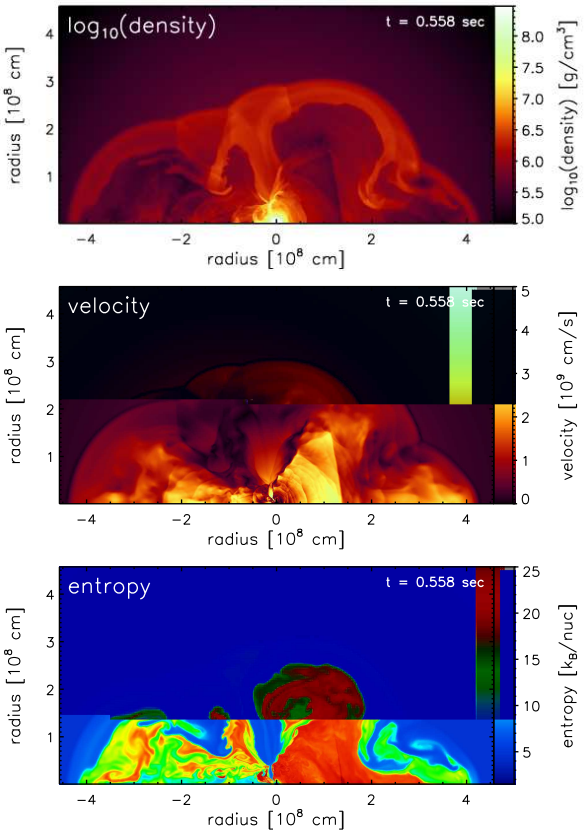

FIGURE 7. Snapshots of density, absolute value of the radial velocity, and entropy per nucleon (from top to bottom) at $\sim$0.56 s after supernova shock formation in one of the explosion simulations of a $15M_{\odot}$ studied in Ref. [34]. The anisotropic density distribution of the ejecta is visible in the upper plot, with mushroom-like Rayleigh-Taylor structures reaching down towards the neutron star at the grid center. The middle panel shows the absolute values of the radial velocity, which reveals strong sonic activity due to the impact of the downflows on the neutron star surface, and the lower plot demonstrates that the outgoing sound waves do not dissipate their energy efficiently in the rapidly expanding neutrino-heated gas so that the entropies of these ejecta are hardly affected.

Alternative explosion mechanisms

Recently, Burrows et al. [21, 22] came up with the suggestion that supernovae might be energized by a strong flux of acoustic power originating from the neutron star. In their 2D simulations they found that the compact remnant is instigated to large-amplitude bipolar oscillations, $l = 1$ core gravity modes, by the anisotropic accretion of gas. The pulsating compact remnant sends pressure waves into its environment, which carry a sizable energy flux and can even steepen into shocks, thus dissipating their energy in the surrounding medium and raising the entropy there. The ringing neutron star acts as a trans-

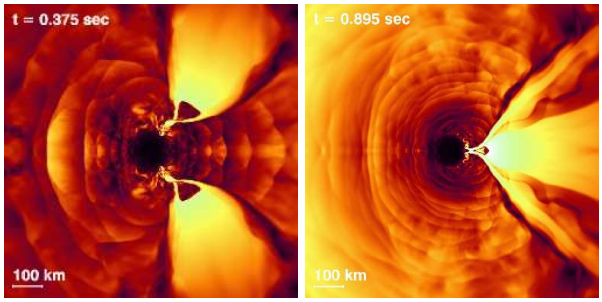

FIGURE 8. Close-up of the neutron star vicinity for two post-bounce times (0.375 s and 0.895 s p.b.) in a simulation like the one shown in Fig. 7. The color coding represents the absolute value of the radial velocity as in the middle panel of the latter figure. The sonic activity by waves emerging from the impact of the accretion flow on the neutron star surface can be particularly well seen in this quantity.

ducer that converts some part of the gravitational binding energy released by the accreted gas into sonic power. The radiated sound was found to be the crucial supply of the developing explosion with energy and momentum and thus triggers acoustically driven explosions.

While this appears as an interesting alternative to initiate the explosion if neutrino heating fails, the question is how the acoustic energy input compares to neutrino heating. Burrows et al. [21] reported that in their simulations the acoustic energy flux dominates the neutrino energy deposition later than several 100 ms after bounce. Although we do not observe the large $l = 1$ core g-modes in the neutron star seen by them at late post-bounce times, and on the basis of our present simulations we can neither judge nor exclude this possibility, also in our models —in the full-scale supernova calculations for $\sim$8–15 $M_\odot$ stars as well as in the parametric explosions— we can clearly identify the presence of strong turbulence in the neutron star surface layer. The gas there is stirred by the violent impact of accretion downflows, thus creating vigorous sonic activity around the neutron star (Figs. 7 and 8). Very approximately, we can estimate the outgoing flux of sonic energy (making the assumptions of spherical symmetry and negligible energy dissipation in the flow) as [36]

$$\begin{aligned} \dot{E}_{\rm sound} &\sim 4\pi r^2 \rho v^2 c_{\rm s} \sim 4\pi r^2 \left(\frac{\rho'}{\rho}\right)^2 \rho c_{\rm s}^3 \\ &\sim 5\times 10^{50}\,\frac{\rm erg}{\rm s}\left(\frac{\rho'}{\rho}\right)^2 , \end{aligned} \qquad (3)$$

where v is the fluid velocity in the sound waves, $c_{\rm s}$ is the sound speed, and ρ'/ρ denotes the amplitude of the ripples on the background density ρ caused by the sound waves. The numerical value in the last expression turns out to be fairly independent of radius and time at some distance from the neutron star in Figs. 7 and 8. For ρ'/ρ of order unity our estimate agrees with values quoted in Burrows et al. [22], which might account for a sizable contribution to the energy of the developing explosion. In our simulations, we indeed see that the perturbations can reach such amplitudes, in particular when the downflow becomes unstable and the perturbations it generates in and around the neutron star surface layer grow. Outside of these transient periods, however, ρ'/ρ is usually significantly smaller. Moreover, the net neutrino energy deposition rates, integrated over the volume of the gain layer, in all of our simulations are typically several 10^{51} erg/s (see Eq. 2), so that the energy input to the explosions in our models is clearly dominated by neutrinos.

Magnetohydrodynamically driven explosions have attracted renewed and increasing interest over the past years for a number of reasons One reason is the discovery of magnetars, which is taken as an indication that at least in some fraction of all cases very strong surface magnetic fields can be generated in neutron stars, possibly already during the evolution phases in which a supernova explosion is triggered. Another reason is the established link of at least some long-duration gamma-ray bursts with very energetic and highly aymmetric hypernova explosions of presumably rapidly rotating massive stars. And a third reason is the interpretation of asymmetries observed in supernova explosions and supernova remnants as consequences and relics of jet-like eruptions or as hints to the ejection of highly collimated material.

Independent of how magnetic fields transfer energy to the explosion, e.g., by hoop stresses, magnetic pressure, or viscous dissipation of energy, the initial magnetic fields in the stellar core must have been amplified during the collapse either by magnetic field wrapping or the magnetorotational instability. Thus they tap the free energy that can be stored in the highly differential rotation of a spinning stellar core that collapses at angular momentum conserving conditions. This free energy, however, is typically a rather small fraction (of order 10%) of the total rotation energy, i.e.,

$$E_{\rm rot}^{\rm free} < E_{\rm rot} \approx 2\times 10^{52}\,{\rm erg}\, M_{\rm ns,1.5} R_{\rm ns,6}^2 \left(\frac{1\,{\rm ms}}{P_{\rm ns}}\right)^2 , \qquad (4)$$

where $R_{\rm ns,6}$ denotes the neutron star radius in 10^6 cm and $P_{\rm ns}$ is the neutron star spin period. A millisecond neutron star typically requires the pre-collapse stellar core to rotate with a period of $P_{\rm ini} \sim P_{\rm ns}(R_{\rm ini}/R_{\rm ns})^2 \sim 10\,{\rm s}\,(P_{\rm ns}/1\,{\rm ms})$. This is significantly faster than predicted by current evolution models for rotating stars, in which the enhanced angular momentum loss due to angular momentum transport by magnetic field effects is taken into account [42]. At the onset of core collapse, the stellar cores are estimated to have spin periods of $P_{\rm ini} > 100\,{\rm s}$ (i.e., $\Omega_{\rm ini} < 0.05\,{\rm rad/s}$). This will lead to neutron stars

with $P_{\rm ns} > 10\,$ms, which is much too slow for rotation to be an energy reservoir of MHD-driven supernovae. Such a conclusion was also reached on the basis of detailed simulations in Refs. [38, 23]. Nevertheless, the MHD mechansim may still need to be invoked for explaining the enormous energy output of long-duration gamma-ray bursts and associated hypernova explosions, which would imply that these events are linked to rare cases where massive stars have achieved to retain a large angular momentum at the time when they end their lives as collapsars [43].

SUMMARY AND OUTLOOK

We have reviewed a variety of recent findings that shed new light on the processes that cause the explosions of massive stars and play a role during the birth of neutron stars. All recent 2D simulations that were performed with a full 180 degree grid agree that the standing accretion shock becomes unstable to low-mode, nonradial deformation. This SASI phenomenon plays a very important role in the supernova core. It was not only found to induce a large asymmetry of the developing blast but also to facilitate neutrino-driven explosions by stretching the time accreted matter can stay in the gain layer and can be exposed to neutrino heating. Moreover, the SASI was observed to excite large-amplitude core g-modes in the neutron star, whose sonic damping could contribute to or be essential for powering the explosion. The asymmetries imprinted on the explosion by the SASI may lateron lead to neutron star kicks and might explain the observed velocities of young pulsars. In three dimensions the $m \neq 0$ modes of the SASI can also have an influence on the spin of the forming neutron star [44].

Despite the general agreement about the importance of the SASI, the physical mechanism behind this phenomenon is still a matter of vivid debate (see [27] and references therein) and the present calculations differ in many conclusions. Partly this is may be so because of the significantly different numerical approaches taken, e.g., regarding the hydrodynamics and neutrino transport, the computational grid, the description of gravity, and the employed equation of state and neutrino interactions. Some of the current discrepancies and controversies, however, will find an explanation when more simulations become available and comparisons are made. Ultimately, however, most of the processes and consequences mentioned above will have to be addressed by 3D models, which are currently still out of reach because of the enormous computational demands of the energy-dependent neutrino transport.

ACKNOWLEDGMENTS

We thank K. Nomoto, A. Heger and S. Woosley for providing us with their progenitor data and are indebted to R. Buras, K. Kifonidis, E. Müller, and M. Rampp for fruitful collaborations. This project was supported by the Deutsche Forschungsgemeinschaft through the Transregional Collaborative Research Centers SFB/TR 27 “Neutrinos and Beyond” and SFB/TR 7 “Gravitational Wave Astronomy”, and the Cluster of Excellence “Origin and Structure of the Universe” (`http://www.universe-cluster.de`). The computations were only possible because of computer time on the IBM p690 of the John von Neumann Institute for Computing (NIC) in Jülich, on the national supercomputer NEC SX-8 at the High Performance Computing Center Stuttgart (HLRS) under grant number SuperN/12758, on the IBM p690 of the Computer Center Garching (RZG), on the sgi Altix 4700 of the Leibniz-Rechenzentrum (LRZ) in Munich, and on the sgi Altix 3700 of the MPI for Astrophysics. We also acknowledge support by AstroGrid-D, a project funded by the German Federal Ministry of Education and Research (BMBF) as part of the D-Grid initiative.

REFERENCES

1. M. Liebendörfer, M. Rampp, H.-Th. Janka, and A. Mezzacappa, *Astrophys. Journal* **620**, 840–860 (2005).
2. M. Liebendörfer, A. Mezzacappa, O.E.B. Messer, G. Martínez-Pinedo, W.R. Hix, and F.-K. Thielemann, *Nuclear Physics* **A719**, 144c–152c (2003).
3. R. Buras, H.-Th. Janka, M. Rampp, and K. Kifonidis, *Astron. Astrophys.* **457**, 281–308 (2006).
4. T.A. Thompson, A. Burrows, and P.A. Pinto, *Astrophys. Journal* **592**, 434–456 (2003).
5. K. Sumiyoshi, S. Yamada, H. Suzuki, H. Shen, S. Chiba, and H. Toki, *Astrophys. Journal* **629**, 922–932 (2005).
6. C.L. Fryer, *Astrophys. Journal* **522**, 413–418 (1999).
7. S.E. Woosley, and A. Heger, *Physics Reports* **442**, 269–283 (2007).
8. S.A. Colgate, and R.H. White, *Astrophys. Journal* **143**, 626–681 (1966).
9. H.A. Bethe, and J.R. Wilson, *Astrophys. Journal* **295**, 14–23 (1985).
10. S.W. Bruenn, and T. Dineva, *Astrophys. Journal* **458**, L71–L74 (1996).
11. L. Dessart, A. Burrows, E. Livne, and C.D. Ott, *Astrophys. Journal* **645**, 534–550 (2006).
12. A. Burrows, L. Dessart, C.D. Ott, and E. Livne, *Physics Reports* **442**, 23–37 (2007).
13. M. Herant, W. Benz, W.R. Hix, C.L. Fryer, and S.A. Colgate, *Astrophys. Journal* **435**, 339–361 (1994).
14. A. Burrows, J. Hayes, and B.A. Fryxell, *Astrophys. Journal* **450**, 830–850 (1995).
15. H.-T. Janka, and E. Müller, *Astron. Astrophys.* **306**, 167–198 (1996).

16. C.L. Fryer, and M.S. Warren, *Astrophys. Journal* **574**, L65–L68 (2002).
17. C.L. Fryer, and M.S. Warren, *Astrophys. Journal* **601**, 391–404 (2004).
18. H.-Th. Janka, K. Langanke, A, Marek, G. Martínez-Pinedo, and B. Müller, *Phys. Reports* **442**, 38–74 (2007).
19. F.S. Kitaura, H.-Th. Janka, and W. Hillebrandt, *Astron. Astrophys.* **450**, 345–350 (2006).
20. E. Livne, A. Burrows, R. Walder, I. Lichtenstadt, and T.A. Thompson, *Astron. Astrophys.* **609**, 277–287 (2004).
21. A. Burrows, E. Livne, L. Dessart, C.D. Ott, and J. Murphy, *Astrophys. Journal* **640**, 878–890 (2006).
22. A. Burrows, E. Livne, L. Dessart, C.D. Ott, and J. Murphy, *Astrophys. Journal* **655**, 416–433 (2007).
23. A. Burrows, L. Dessart, E. Livne, C.D. Ott, and J. Murphy, *Astrophys. Journal* **664**, 416–434 (2007).
24. M. Rampp, and H.-Th. Janka, *Astron. Astrophys.* **396**, 361–392 (2002).
25. R. Buras, M. Rampp, H.-Th. Janka, and K. Kifonidis, *Astron. Astrophys.* **447**, 1049–1092 (2006).
26. T. Foglizzo, L. Scheck, and H.-Th. Janka, *Astrophys. Journal* **652**, 1436–1450 (2006).
27. L. Scheck, H.-Th. Janka, T. Foglizzo, and K. Kifonidis, arXiv:0704.3001, *Astron. Astrophys.*, in press (2007).
28. J.M. Blondin, A. Mezzacappa, and C. DeMarino, *Astrophys. Journal* **584**, 971–980 (2003).
29. T. Yamasaki, and S. Yamada, *Astrophys. Journal* **656**, 1019–1037 (2007).
30. N. Ohnishi, K. Kotake, and S. Yamada, *Astrophys. Journal* **641**, 1018–1028 (2006).
31. J.M. Blondin, and A. Mezzacappa, *Astrophys. Journal* **642**, 401–409 (2006).
32. A. Marek, and H.-Th. Janka, arXiv:0708.3372, *Astrophys. Journal*, submitted (2007).
33. S.W. Bruenn, C.J. Dirk, A. Mezzacappa, et al., "Modeling Core Collapse Supernovae in 2 and 3 Dimensions with Spectral Neutrino Transport," in *SciDAC 2006, Scientific Discovery through Advanced Computing*, edited by W.M. Tang, et al., Journ. Phys. Conf. Ser. 46, 2006, pp. 393–402; arXiv0709.0537.
34. L. Scheck, K. Kifonidis, H.-Th. Janka, and E. Müller, *Astron. Astrophys.* **457**, 963–986 (2006).
35. K. Kifonidis, T. Plewa, L. Scheck, H.-Th. Janka, and E. Müller, *Astron. Astrophys.* **453**, 661–678 (2006).
36. L.D. Landau, and E.M. Lifschitz, *Hydrodynamik*, Akademie Verlag, Berlin, 1991, pp. 325–330.
37. S. Akiyama, J.C. Wheeler, D.L. Meier, and I. Lichtenstadt, *Astrophys. Journal* **584**, 954–970 (2003).
38. T.A. Thompson, E. Quataert, and A. Burrows, *Astrophys. Journal* **620**, 861–877 (2005).
39. T. Takiwaki, K. Kotake, and K. Sato, arXiv:0712.1949, *Astrophys. Journal*, submitted (2007).
40. M. Obergaulinger, M.A. Aloy, H. Dimmelmeier, and E. Müller, *Astron. Astrophys.* **457**, 209–222 (2006).
41. S.G. Moiseenko, and G.S. Bisnovatyi-Kogan, *Astrophysics and Space Science* **311**, 191–195 (2007).
42. A. Heger, S.E. Woosley, and H.C. Spruit, *Astrophys. Journal* **626**, 350–363 (2005).
43. A.I. MacFadyen, S.E. Woosley, *Astrophys. Journal* **524**, 262–289 (1999).
44. J.M. Blondin, and A. Mezzacappa, *Nature* **445**, 58–60 (2007).